IEEE Access
Multidisciplinary ⋮ Rapid Review ⋮ Open Access Journal

Received May 30, 2019, accepted June 19, 2019, date of publication June 26, 2019, date of current version July 18, 2019.

Digital Object Identifier 10.1109/ACCESS.2019.2925073

V-Band End-Fire Radiating Planar Micromachined Helical Antenna Using Through-Glass Silicon Via (TGSV) Technology

AQEEL HUSSAIN NAQVI, (Student Member, IEEE), JEONG-HEUM PARK, CHANG-WOOK BAEK, (Member, IEEE), AND SUNGJOON LIM, (Member, IEEE)
School of Electrical and Electronics Engineering, Chung-Ang University, Seoul 06974, South Korea

Corresponding authors: Chang-Wook Baek (cwbaek@cau.ac.kr) and Sungjoon Lim (sungjoon@cau.ac.kr)

This work was supported by the National Research Foundation of Korea (NRF) funded by the Korea government (MOE) (2017R1D1A1B03029995) and (MSIT) (2018R1A4A1023826).

ABSTRACT In this paper, we demonstrate a V-band planar micromachined helical antenna (PHA) with end-fire radiation on the glass substrate. The planar rectangular helical configuration is realized using the novel through-glass silicon via (TGSV) technology. The proposed micromachined antenna is designed and fabricated on a borosilicate glass substrate of thickness 350 μm, which has a very low-dielectric loss compared to silicon at millimeter-wave bands. The proposed PHA is fed by a microstrip line, and the planar helical configuration with 3.25 turns with a truncated ground plane is designed for achieving wideband end-fire radiation with seven tungsten-coated silicon vias and six connected gold arm patterns, which are fabricated using the TGSV technology. The electrical length of the proposed antenna is ($3\ \lambda_0 \times 1.4\ \lambda_0$). The designed antenna operates at the center frequency of 58 GHz. A prototype of the proposed antenna is fabricated by micromachining technology and tested. The simulated and measured results show that the proposed antenna has a wide operational bandwidth of 50.3 to 65 GHz for $|S_{11}| < -10$ dB with a fractional bandwidth (FBW) of 25.5%. The measured peak gain is 6.3 dBi, and measured efficiency is 62% at the center frequency of 58 GHz. All measurements are in close agreement with simulated results. The proposed planar helical antenna with end-fire radiation is useful for applications in traveling-wave-tubes operating in millimeter-wave and higher frequencies, millimeter-wave on-board wireless communication, radar imaging, and tracking applications.

INDEX TERMS Borosilicate-glass, end-fire, planar helical antenna, through glass silicon via (TGSV), travelling-wave-tubes (TWTs).

I. INTRODUCTION

In the past few decades, the emergence of new generations in communication technology has greatly affected the routine and daily lives of people and resulted in the gradual increase in data traffic and number of communication devices [1]–[5]. Various types of wireless services have been introduced and developed with the rapid growth of wireless communication techniques [6]–[10]. The use of unused frequency spectra is highly focused due to the increasing requirement of high data rates in wireless communication [11]. Millimeter-wave communication, which is also referred to as the 5th-generation (5G) wireless communication, has attracted significant attention and is expected to be implemented by the early 2020s. Compared to 4G, 5G wireless communication has different performance metrics that require data rates of the order of gigabits per second (Gbps), millisecond-level delay, enhanced spectral energy and enhanced cost factor. At high frequencies, the signal-to-interference-plus-noise ratio (SINR) is generally known to considerably decrease due to the extreme free space loss and blockage experienced by electromagnetic waves. The use of highly directional antennas and line-of-sight (LOS) communication can greatly alleviate these problems [1].

Because of the increasing amount of data streaming, video calling, high definition television (HDTV) and video gaming, a big challenge for the industry is the increasing demand of high Gbps data rates. Utilization of millimeter-wave

The associate editor coordinating the review of this manuscript and approving it for publication was Qingfeng Zhang.

 This work is licensed under a Creative Commons Attribution 3.0 License. For more information, see http://creativecommons.org/licenses/by/3.0/

communication is an attractive option to fulfill this high demand. With the increasing input/output (I/O) numbers of integrated circuits (ICs) in millimeter-wave communication systems [12], through-substrate vias [13], [14] are becoming essential for the small-footprint, high-density, low-power three-dimensional (3D) stacking integration in advanced electronic systems. Over the last few years, silicon interposers with through-silicon vias (TSVs) have been numerously reported as an alternative for the conventional organic substrates [13], [14] due to their advantages such as shorter signal paths, ease of wafer processing and die-matched coefficient of thermal expansion (CTE). However, silicon interposers with TSV technologies have challenges such as the fabrication cost, process complexity and high electrical substrate losses. Recently, glass interposers with through-glass vias (TGVs) have been extensively studied [15]–[18] because of their excellent electrical properties as low substrate losses at high frequency, CTE adjustability, fine line spacing, availability of large and ultra-thin panels, low material and manufacturing cost [19]. Based on these merits, glass interposers are the best alternative for conventional silicon interposers and an attractive platform for high frequency, radio frequency (RF), microwave passive components and packaging [20]–[22].

Among various types of antennas reported in the literature, helical antennas exhibit high gain, high directivity and wide bandwidth, which make them highly useful for airborne and tracking applications [3], [23]–[26]. However, the conventional helical antennas are not suitable for surface-mounted applications due to space constraints because helical antennas generally have a high profile. Based on the merits of the helical antenna structure, many studies have been conducted to design a low-profile and compact helical antenna. In [27], a hemispherical helical structure is used to realize a compact and low-profile structure. In [25], a meander line technique is used to design a compact printed quadrifilar helical antenna by decreasing the length of the antenna. From a practical viewpoint, a planar helix structure is the best choice to install as either square or rectangular structures. A rectangular helix structure further reduces the profile of the antenna to be more compact. In [24], a planar rectangular helical structure has been realized on a duroid substrate using plated via holes to achieve circularly polarized radiation. Furthermore, a rectangular planar helix structure is the best candidate for applications with slow-wave structures and linearly polarized antennas.

In this paper, a V-band planar micromachined helical antenna (PHA) with end-fire radiation is demonstrated on the glass substrate. The planar rectangular helical configuration is realized using the novel through-glass silicon via (TGSV) technology as shown in Fig. 1. The proposed antenna is designed and fabricated on a borosilicate glass substrate of thickness 350 μm, which has a very low dielectric loss compared to silicon at the millimeter-wave bands. The metal-coated TGSVs in this work, which are fabricated by the micromachining technology based on deep

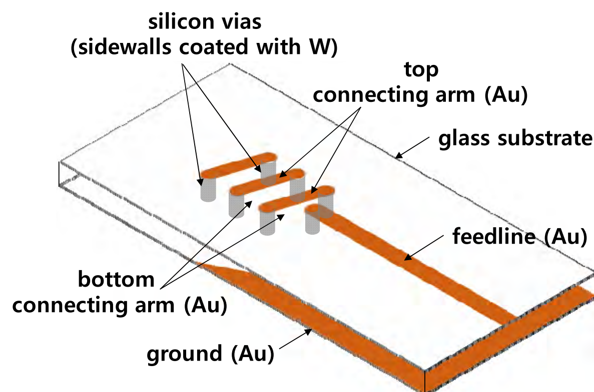

FIGURE 1. Prospective view of the proposed antenna.

silicon etching and glass reflow, can effectively substitute for completely-filled metallic vias in the conventional TGVs without degrading the performance of the antenna. The performance of the proposed antenna will be numerically and experimentally demonstrated.

The remainder of the paper has been organized as follows. The design of the planar helical antenna is described in Section II. In Section III, the fabrication process is explained in detail. Section IV discusses the simulated and experimental results of the proposed antenna. Finally, conclusions are drawn in Section V with the advantages of the proposed research work.

II. ANTENNA DESIGN

A helix antenna is a hybrid of two conventional radiating elements: a dipole and a loop antenna. The helix becomes a dipole antenna when the diameter of the helix approaches zero, or the pitch angle becomes 90°. Moreover, a helix with a uniform diameter becomes a loop antenna if the spacing between the helix turns becomes zero. In the last few decades, due to the unique and extraordinary properties of the helix antennas, they were extensively used as simple radiators. The conventional circular helix has two radiation modes: normal mode and axial mode. In the axial mode of operation, the helix can achieve a narrow beam along the helix axis over a wide range of frequencies. Because of these properties, helical antennas continue to be a topic of research these days. Although the conventional circular helix has the space constraints and is difficult to fabricate through printed-circuit or micromachining process, the printed-circuit technology has the advantages of miniaturization, low-cost and large-scale fabrication. Meanwhile, the microfabrication technology is becoming a key interest as future wireless communication is shifting to higher frequencies of operation, where the dimensions become small. Hence, the microfabrication technology has become a key interest of research.

The proposed antenna has been designed based on the design principle of the conventional helical antenna in the axial mode. In the remainder of the paper, PHA is referred to as the proposed planar helical antenna. The PHA has a few

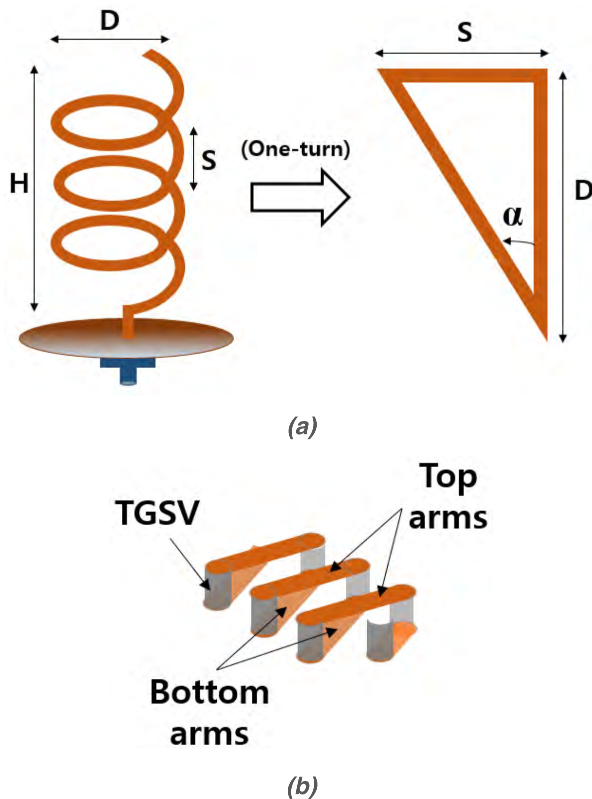

FIGURE 2. (a) Geometry and dimensions of the conventional helical antenna (left) and one uncoiled turn of the helix (right). (b) Perspective view of geometry of the planar helix.

advantages such as: 1) it has a low-profile and is very suitable to be installed on satellites and spacecrafts, 2) it can achieve a wide impedance bandwidth like conventional circular helix with an end-fire radiation in the operational frequency band, 3) the structure is simple, lightweight and low-cost. Hence, the proposed PHA retains the property of the conventional circular helix as broad-band and end-fire radiation. The PHA is designed on an ultra-thin borosilicate glass substrate with a permittivity and a tangent loss of 4.6 and 0.0037, respectively. The glass substrate is 350 μm thick. When a single turn of the helix is uncoiled, as shown in Fig. 2(a), it reveals the parameters of the helix in planar structure as follows [23]:

$D =$ Diameter of helix,

$C =$ Circumference of helix; $C = \pi D$,

$S =$ Spacing between helix turns,

$L =$ Length of one turn; $L = \sqrt{C^2 + S^2}$,

$\alpha =$ Pitch angle; $\alpha = \sin^{-1} \frac{S}{L}$,

where D is transformed to an arm-length of the planar helix, C is transformed to the total length of one turn helix, α is the pitch angle between the top and bottom arms. The top and bottom arms have achieved diagonal edge connections through vias. A perspective view of geometry of PHA is shown in Fig. 2(b).

To design PHA, we first calculated the nominal design parameters of the conventional helix at the operating frequency of 60 GHz. According to [23], the helix can achieve a wide operating bandwidth with end-fire radiation if it satisfies the criteria of 3/4 $< C/\lambda <$ 4/3. Hence, we selected $C/\lambda = 1$, the number of turns is $N = 3.25$, and the spacing between the helix turns is $S = \lambda/4$. Therefore, circumference C of the 1-turn helix is equal to the free-space wavelength λ_o at 60 GHz frequency; α is the calculated pitch angle of the top and bottom arms and is equal to 18°. The top and bottom arms are connected with each other through vias, which are called TGSVs.

A parametric study was conducted to analyze the effects of these key design parameters on the radiation performance and impedance matching to reach the practical design of PHA with low-profile and end-fire radiation. The key design parameters are: number of helical turns (N) and pitch angle (α) between the top and bottom helical arms, and bottom ground plane.

With these nominal design parameters as the starting point, the 1.25-turn helix with a simple partial ground has been designed as shown in Fig. 3(a). Pitch angle α plays an important role in the current distribution on upper and lower helical arms. It is observed that peak gain is 3.12, 4.55 and 3.19 dBi for angle $\alpha = 16^{\circ}$, 18° and 20°, respectively. Since current distribution on the strips is in x- and y-directed components, and larger α increases the current distribution in the y-direction, thus increasing the side-lobe level. Therefore, we chose $\alpha = 18^{\circ}$ in our proposed design with a 10-dB impedance matching of 51.4–55.1 GHz and a peak gain of 4.55 dBi in the end-fire direction. To enhance the gain, the helical turn is increased as shown in Fig. 3(b). It is observed that the peak gain is increased from 4.55 dBi (Stage-1: $N = 1.25$) to 7.18 dBi (Stage-3: $N = 3.25$) by introducing two more helical turns. Next, the simple partial ground (Stage-3: $N = 3.25$) was further modified to form a U-shaped horizontal ground plane with a truncated slot in the middle (Stage-4: $N = 3.25$) to achieve a broadband 10-dB impedance matching from 50.7 to 65.8 GHz and increase the gain to 7.89 dBi. The reflection coefficients are almost not changed at different number of turns N as shown in Fig. 3(c). However, the radiation pattern becomes more directional at larger N as shown in Fig. 3(b).

Figure 4 shows the final design of the proposed PHA. To achieve the maximum radiation along the axis of the helix, i.e., in the end-fire direction, a 3.25-turn helix is designed as shown in Fig. 4(a). A U-shaped metallic gold plate is patterned on the back side of the glass substrate to form a horizontal ground plane. The U-shaped ground wall helps to increase the gain in the end-fire direction and improve the radiation pattern as shown in Fig. 3(b). A truncated slot is introduced in the middle of the ground plane to achieve a broadband impedance matching over the V-band as observed from Fig. 3(c). A microstrip feed line is used to feed the helix with a modified ground plane as shown in Fig. 4(a). A straight edge via connection called as TGSV is used for the electrical interconnection between the top and bottom helical arms as shown in Fig. 4(c). All TGSVs have identical heights, which are equal to the substrate thickness, and identical diameters,

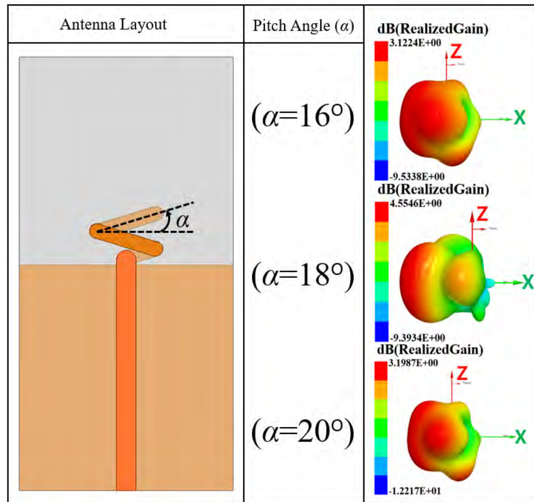

(a)

Design Description	Antenna Layout	3D-Radiation Pattern
Stage-1: N=1.25 turns α=18° GND=Simple Ground		dB(RealizedGain) 4.5546E+00 … -9.3934E+00
Stage-2: N=2.25 turns α=18° GND=Simple Ground		dB(RealizedGain) 5.6521E+00 … -1.0170E+01
Stage-3: N=3.25 turns α=18° GND=Simple Ground		dB(RealizedGain) 7.1843E+00 … -1.2743E+01
Stage-4: N=3.25 turns α=18° GND=Truncated GND		dB(RealizedGain) 7.8942E+00 … -1.2990E+01

(b)

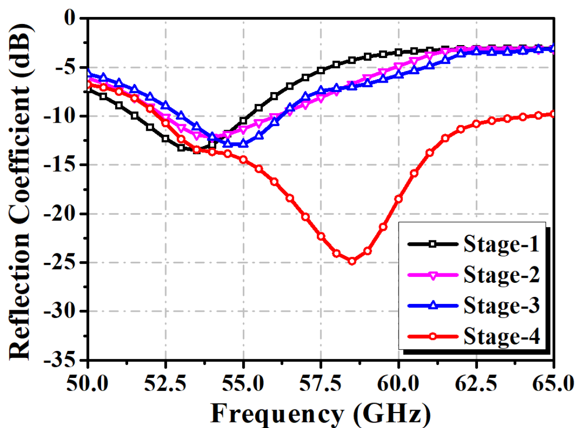

(c)

FIGURE 3. (a) 3-D radiation pattern for different pitch angle α, (b) design iterations of the proposed planar helical antenna, and (c) reflection coefficient plot for various design iterations.

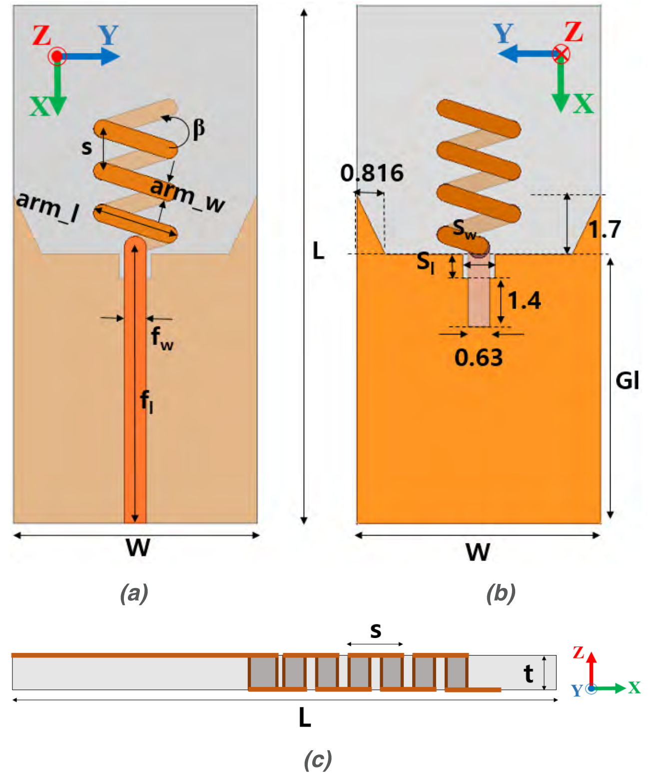

FIGURE 4. (a) Top and (b) bottom view of the proposed planar helical antenna. (c) Side view of the proposed antenna.

TABLE 1. Dimensions of the planar helical antenna (unit: Millimeters).

Parameter	L	W	S_w	S_l	F_w	F_l
Value (mm)	15	7	0.9	0.7	0.627	8
Parameter	arm_l	arm_w	Gl	t	s	β
Value (mm)	2	0.5	7.8	0.35	1.2	36 deg

which are equal to the width of the arm. The side wall of the silicon vias are coated with a thin layer of tungsten metal, whereas the top and bottom arms are patterned with gold. The final geometrical parameters are listed in Table 1. Figures. 5(a), (b), (c) and (d) show the simulated 3-D radiation patterns at 54, 56, 58 and 60 GHz, respectively. The peak gain at 54, 56, 58 and 60 GHz is 7.95, 7.89, 7.42, and 6.44 dBi, respectively.

The complete design procedure of the PHA can be summarized as follows:

1) Compute the circumference of the circular helix and calculate length L of the top and bottom arms of the PHA.
2) Tilt both arms of the top and bottom sides at an angle equal to pitch angle α in the opposite direction.
3) Design a via of height t, which is equal to the thickness of the substrate, and connect the top and bottom arms through the via.

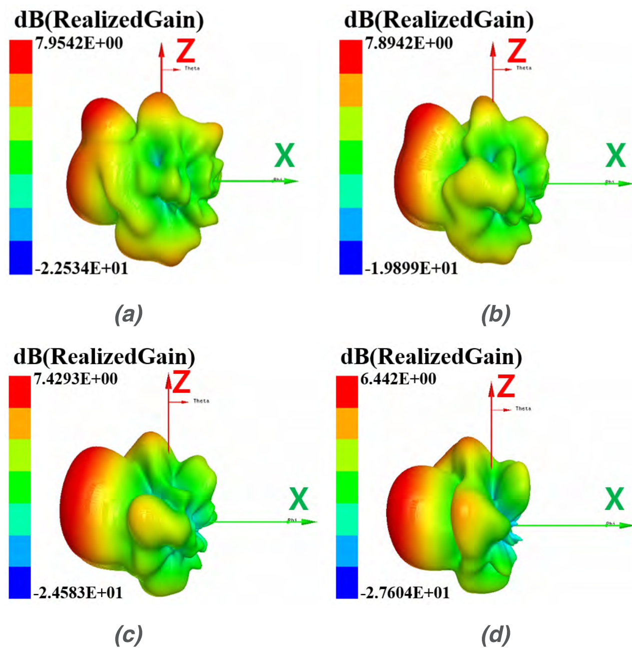

FIGURE 5. Simulated 3-D far-field radiation patterns: (a) 54 GHz, (b) 56 GHz, (c) 58 GHz, and (d) 60 GHz.

4) Design a feeding by choosing a proper feeding technique. We selected a microstrip feed followed by a V-band connector.
5) Design a U-shaped modified ground plane to achieve the best impedance matching over a wide range of frequencies.
6) Optimize the design parameters with respect to the end-fire radiation and peak gain.

The proposed antenna has been designed and verified using the ANSYS high-frequency structure simulator (HFSS) [28].

III. ANTENNA FABRICATION

The proposed planar helical antenna was fabricated using the TGSV technology based on the deep reactive ion etching (DRIE) of silicon, selective metal coating and glass reflow processes, which are similar to the process developed in our group [2]. The overall fabrication process of the proposed planar helical antenna is shown in Fig. 6. The process began with the first short DRIE of silicon using a photolithographically-patterned photoresist mask (AZ P4330-RS) to form a 3-μm-deep shallow cavity near the silicon via regions (Fig. 6(a)). A 4-inch, 525-μm-thick, boron-doped p-type low-resistive silicon wafer with a resistivity of 0.01∼0.02 Ω·cm was used to minimize the via loss. After the photoresist had been removed in acetone, a 0.2-μm-thick aluminum layer was evaporated and patterned inside the cavity by wet etching with a PAN solution, which is a mixture of phosphoric, acetic and nitric acids in the ratio of 16:1:1 using a photoresist mask. Then, the second DRIE of silicon was performed to define a 370-μm-deep trench for the glass reflow region, and the silicon vias of identical

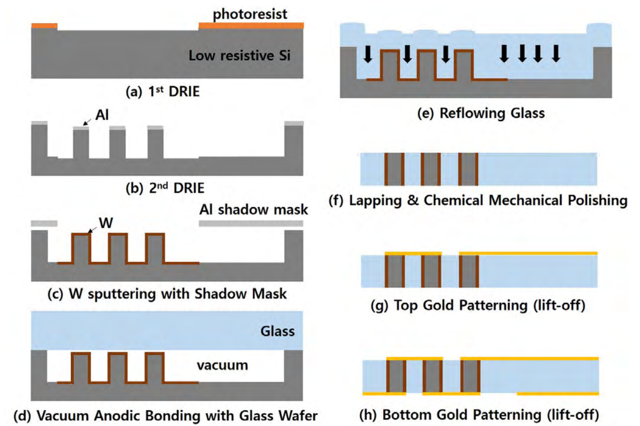

FIGURE 6. Overall fabrication process flow of the proposed antenna.

heights inside the trench, using the patterned aluminum layer as an etch mask (Fig. 6(b)). After the aluminum had been stripped off, a 0.5-μm-thick tungsten layer was selectively coated on the silicon vias by sputtering using an aluminum shadow mask (Fig. 6(c)).

Then, this substrate was anodically bonded with a 4-inch, 525-μm-thick borosilicate glass wafer (BOROFLOAT® 33, SCHOTT AG, Mainz, Germany) in a vacuum environment (Fig. 6(d)). Due to the shallow cavity formed in the first step, the tungsten layers on the top surface of the silicon vias do not touch the glass wafer during the anodic bonding process. The glass reflow was performed by putting the wafer stack into a furnace, heating to 800 °C, holding for 8 hours and cooling to the room temperature. During this step, the glass was melted and flowed into the silicon trench due to the lower pressure in the sealed trench than the atmospheric pressure (Fig. 6(e)). We used tungsten metal to coat the vias because of the high temperature of the glass reflow process, since tungsten has a higher melting point (3422 °C) than other conductive metals and can withstand this high temperature without deforming or changing the state. Then, both sides of the substrate were planarized by mechanically lapping and polishing using a CMP (chemical mechanical polishing) process (Fig. 6(f)). The overfilled glass on the front surface was ground and carefully polished until the surface of the silicon via was exposed; then, the remaining silicon and glass at the backside were ground and polished together until the entire substrate became 350 μm thick. At this stage, both top and bottom surfaces of the silicon vias were completely exposed.

Finally, the helical arms and microstrip feedlines were patterned on the top side of the substrate by evaporating and patterning a chromium (10 nm)/gold (300 nm) metal layer using a lift-off process with an image reversal photoresist (AZ5214E) (Fig. 6(g)). On the backside of the substrate, the helical arms and ground were patterned using the same process (Fig. 6(h)). The top and back sides of the fabricated prototype of PHA are shown in Figs. 7(a) and (b). The fabricated prototype was mounted on a V-band endlaunch connector by Southwest Company for measurements as shown in Fig. 7(c).

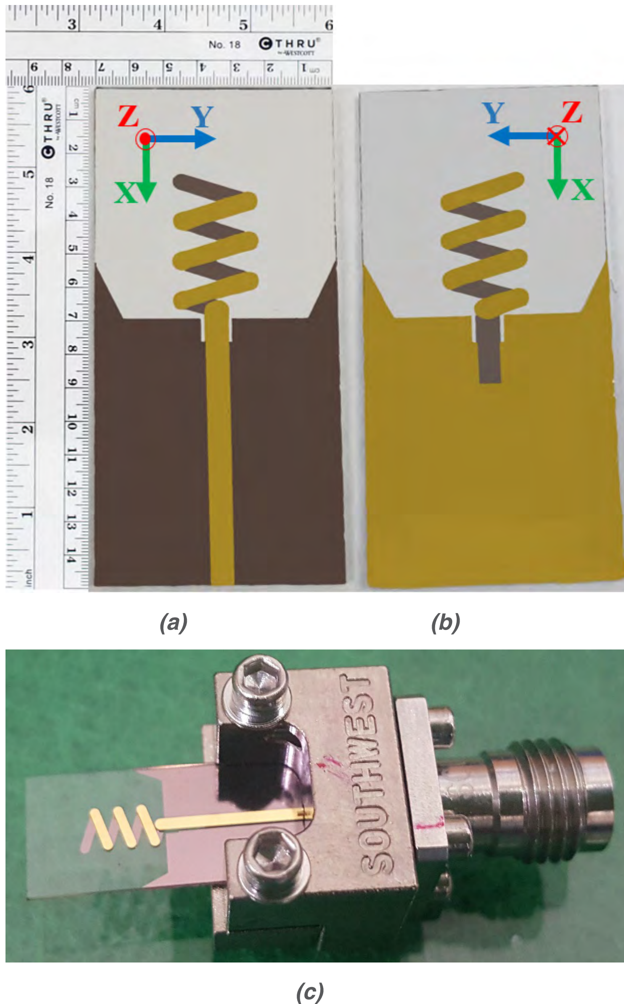

FIGURE 7. Photos of the final fabricated prototype of the proposed planar helical antenna: (a) Top view, (b) bottom view, and (c) antenna with the V-band connector.

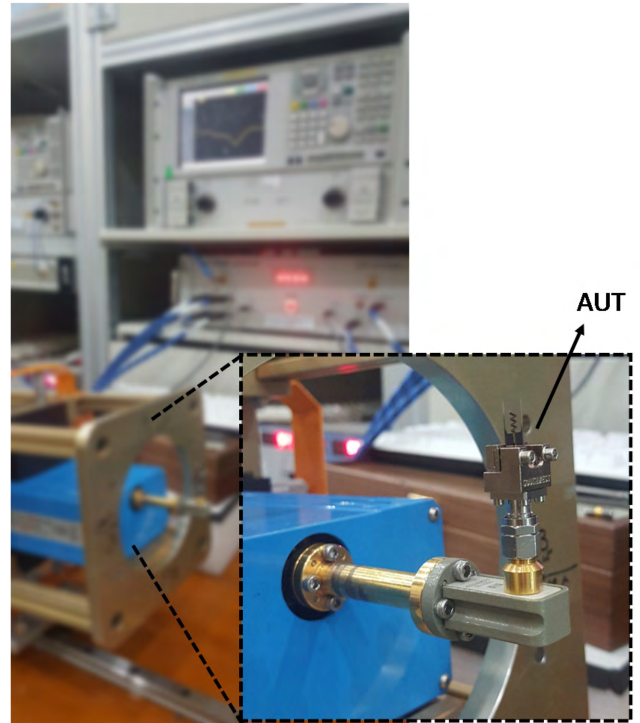

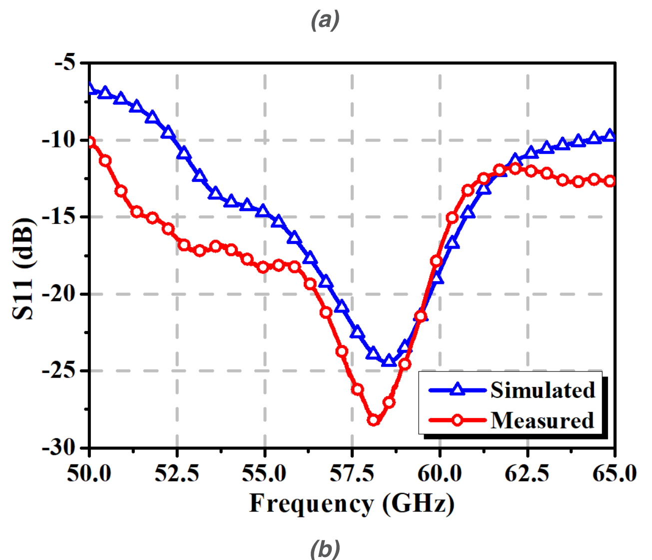

FIGURE 8. (a) S-parameter measurement setup and (b) simulated and measured reflection coefficient plots.

IV. MEASUREMENT RESULTS AND DISCUSSION

A. S-PARAMETER MEASUREMENTS

The S-parameters of the fabricated prototype were measured using a calibrated Agilent network analyzer N5260A (Keysight Technologies Corporation, Morgan Hill, CA, USA), as shown in Fig. 8(a).

Figure 8(b) shows the comparison of the simulated and measured S-parameters of the fabricated PHA. The measured 10-dB impedance bandwidth is 50.3–65 GHz, and the simulated 10-dB impedance bandwidths is 52.17–64.10 GHz.

The measured 10-dB fractional impedance bandwidth is 25.5%. Thus, the simulated and measured S-parameters are consistent with each other.

B. RADIATION PATTERN MEASUREMENTS

The far-field radiation pattern of the fabricated antenna prototype is measured using the commercial ORBIT/FR far-field measurement system in a shielded millimeter-wave anechoic chamber, as shown in Fig. 9(a). The transmit horn antenna is the SGH-series (SGH-15) by Millitech Company, which has a standard gain of 24 dBi. Figures. 9(b), (c), (d), and (e) show the measured and simulated 2-D radiation patterns in the azimuth plane (XY plane) at frequencies of 54, 56, 58, and 60 GHz (the range of the 10-dB impedance bandwidth), respectively. The measured peak gains of the antenna at 54, 56, 58, and 60 GHz are 4.9 dBi, 5.5 dBi, 6.3 dBi, and 5.3 dBi, respectively, while the simulated peak gains are 6 dBi, 7.9 dBi, 7.4 dBi, and 6.5 dBi. The simulated and measured peak gain plot of the proposed antenna is shown in Fig. 10(a). The measured radiation efficiency of the antenna is calculated

TABLE 2. State-of-the-art performance comparison.

Ref. #	Type of Substrate	Fabrication Technology	Antenna Type	Operating Frequency Band	Height	Peak Gain (dBi)	Electrical Size
[4]	Epoxy & Glass Cloth Resin	PCB	MSL-to-Waveguide	V-band	$0.2\lambda_o$	2.2	$0.96\lambda_o\times1.28\lambda_o$
[15]	Glass	TGV	Via-Monopole	W-band	$0.1\lambda o$	1.23	$0.75\lambda o\times0.75\lambda o$
[19]	Glass	Panel-based Double-side Thin-film Processing	Yagi-Uda	V-band	$0.04\ \lambda_o$	3.1	$0.5\lambda_o\times0.5\lambda_o$
[24]	RT Duroid 5880	Plated via-holes	Planar Helical	X-band	$0.11\lambda_o$	10.5	$1.23\lambda_o\times0.77\lambda_o$
This Work	**Borosilicate Glass**	**Micromachining (TGSV)**	**Planar Helical**	**V-band**	$\mathbf{0.07\lambda_o}$	**6.3**	$\mathbf{3\lambda_o\times1.4\lambda_o}$

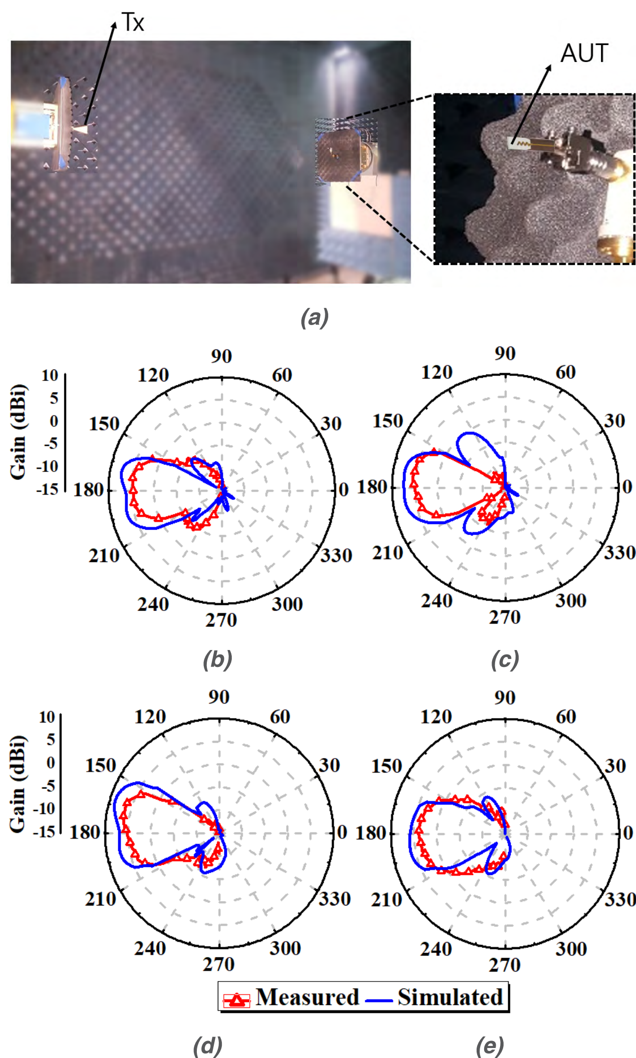

FIGURE 9. (a) Photo of the radiation pattern measurement setup. Measured 2-D far-field radiation patterns on XY plane: (b) 54 GHz, (c) 56 GHz, (d) 58 GHz, and (e) 60 GHz.

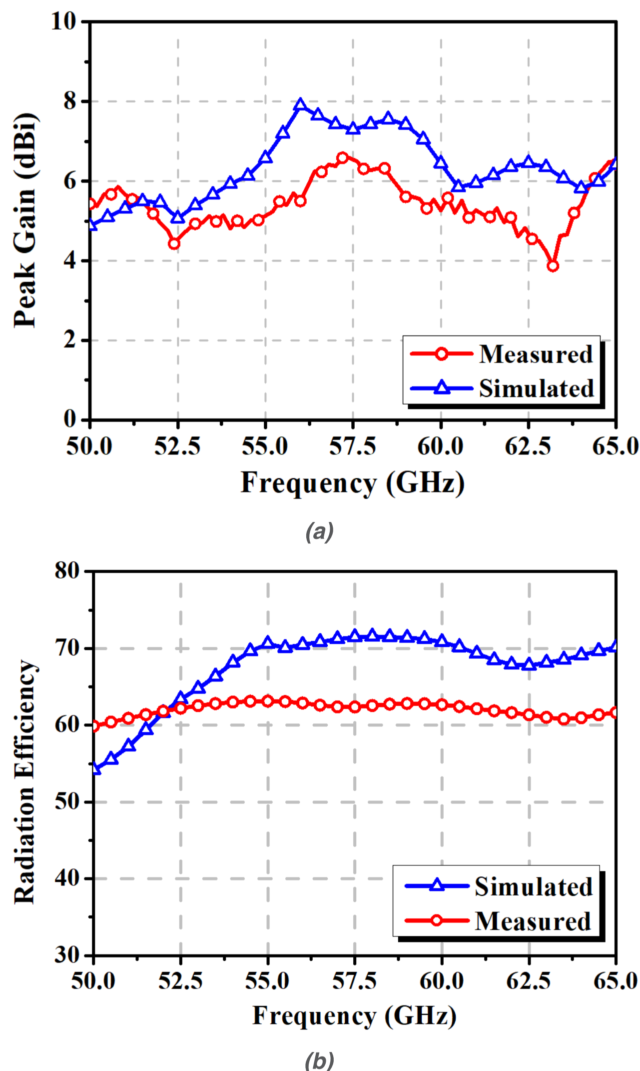

FIGURE 10. (a) Simulated and measured peak gain versus frequency. (b) Simulated and measured radiation efficiency plot versus frequency.

from the ratio of the measured peak gain to the simulated directivity. The measured radiation efficiency of the antenna at 54, 56, 58, and 60 GHz is 63, 62, 62, and 63%, respectively, while the simulated radiation efficiency is 68, 71, 72, and 71%. The simulated and measured radiation efficiency plot of the proposed antenna is shown in Fig. 10(b). The measured

peak gain and radiation efficiency are slightly lower than simulated results because dielectric loss of a glass substrate is larger with higher frequencies. Table 2 contains a performance comparison of state-of-the-art antennas with the proposed work in terms of antenna design type, operational frequency band, fabrication technique, peak gain, substrate height and antenna size.

V. CONCLUSION

This paper presents a V-band end-fire radiated planar helical antenna on an ultrathin (350 μm) borosilicate glass substrate using tungsten-coated TGSV processes. The measured performance shows good preliminary results with a 10-dB fractional bandwidth of 25.5% and a measured gain of 6.3 dBi at 58 GHz frequency in the V-band. The simulated and measured results are consistent with each other. The proposed work paves the way for the development of millimeter-wave antennas and modules on an ultra-thin glass substrate using the wafer-level, batch-processing microfabrication technology.

REFERENCES

[1] A. H. Naqvi and S. Lim, "Review of recent phased arrays for millimeter-wave wireless communication," *Sensors*, vol. 18, no. 10, p. 3194, 2018.

[2] I.-J. Hyeon and C.-W. Baek, "Millimeter-wave substrate integrated waveguide using micromachined tungsten-coated through glass silicon via structures," *Micromachines*, vol. 9, no. 4, p. 172, Apr. 2018.

[3] X. Tang, Y. He, and B. Feng, "Design of a wideband circularly polarized strip-helical antenna with a parasitic patch," *IEEE Access*, vol. 4, pp. 7728–7735, 2016.

[4] R. Suga, H. Nakano, Y. Hirachi, J. Hirokawa, and M. Ando, "Cost-effective 60-GHz antenna package with end-fire radiation for wireless file-transfer system," *IEEE Trans. Microw. Theory Techn.*, vol. 58, no. 12, pp. 3989–3995, Dec. 2010.

[5] Y. Li and K.-M. Luk, "A multibeam end-fire magnetoelectric dipole antenna array for millimeter-wave applications," *IEEE Trans. Antennas Propag.*, vol. 64, no. 7, pp. 2894–2904, Jul. 2016.

[6] M. J. Marcus, "5G and "IMT for 2020 and beyond" [Spectrum policy and regulatory issues]," *IEEE Wireless Commun.*, vol. 22, no. 4, pp. 2–3, Aug. 2015.

[7] M. Cai, J. N. Laneman, and B. Hochwald, "Carrier aggregation for phased-array analog beamforming with beam squint," in *Proc. IEEE Global Commun. Conf. (GLOBECOM)*, Singapore, Dec. 2018, pp. 1–7.

[8] W. Hong, S.-T. Ko, Y. Lee, and K.-H. Baek, "Compact 28 GHz antenna array with full polarization flexibility under yaw, pitch, roll motions," in *Proc. 9th Eur. Conf. Antennas Propag. (EuCAP)*, Lisbon, Portugal, Apr. 2015, pp. 1–3.

[9] D. M. Pozar, *Microwave Engineering*, 3rd ed. Hoboken, NJ, USA: Wiley, 2005.

[10] J. J. H. Wang, "Wideband wide-scan millimeter-wave phased arrays for enhanced security/privacy and performance in 5G mobile wireless," in *Proc. IEEE Int. Symp. Antennas Propag. USNC/URSI Nat. Radio Sci. Meeting*, San Diego, CA, USA, pp. 1471–1472, Jul. 2017.

[11] C. Dehos, J. L. González, A. De Domenico, D. Kténas, and L. Dussopt, "Millimeter-wave access and backhauling: The solution to the exponential data traffic increase in 5G mobile communications systems?" *IEEE Commun. Mag.*, vol. 52, no. 9, pp. 88–95, Sep. 2014.

[12] G. M. Rebeiz, "Millimeter-wave large-scale phased-arrays for 5G systems," in *IEEE MTT-S Int. Microw. Symp. Dig.*, Phoenix, AZ, USA, pp. 28–30, May 2015.

[13] J. Leib and M. Topper, "New wafer-level-packaging technology using silicon-via-contacts for optical and other sensor applications," in *Proc. 54th Electron. Compon. Technol. Conf.*, Jun. 2004, pp. 843–847.

[14] M. Sunohara, T. Tokunaga, T. Kurihara, and M. Higashi, "Silicon interposer with TSVs (through silicon vias) and fine multilayer wiring," in *Proc. 58th Electron. Compon. Technol. Conf.*, May 2008, pp. 847–852.

[15] S. Hwangbo, A. Rahimi, C. Kim, H.-Y. Yang, and Y.-K. Yoon, "Through Glass Via (TGV) disc loaded monopole antennas for millimeter-wave wireless interposer communication," in *Proc. IEEE 65th Electron. Compon. Technol. Conf. (ECTC)*, May 2015, pp. 999–1004.

[16] Y. Jun, S. Ma, F. Ma, Y. Xia, R. Luo, Y. Jin, and J. Chen, "Process development of through-glass-via (TGV) interposer for radio frequency (RF) applications," in *IEEE MTT-S Int. Microw. Symp. Dig.*, Jul. 2016, pp. 1–4.

[17] S. Hwangbo, A. B. Shorey, and Y.-K. Yoon, "Millimeter-wave wireless intra-/inter chip communications in 3D integrated circuits using through glass via (TGV) disc-loaded patch antennas," in *Proc. IEEE 66th Electron. Compon. Technol. Conf. (ECTC)*, Las Vegas, NV, USA , pp. 2507–2512, May/Jun. 2016.

[18] M. Töpper, "3-D thin film interposer based on TGV (through glass vias): An alternative to Si-interposer," in *Proc. 60th Electron. Compon. Technol. Conf. (ECTC)*, Jun. 2010, pp. 66–73.

[19] W. T. Khan, S. Sitaraman, A. L. Vera, M. R. Pulugurtha, V. Sundaram, R. R. Tummala, J. Papapolymerou, "A V-band end-fire Yagi-Uda antenna on an ultra-thin glass packaging technology," in *Proc. Eur. Microw. Conf. (EuMC)*, Sep. 2015, pp. 618–621.

[20] R. Ostholt, N. Ambrosius, and R. A. Krüger, "High speed through glass via manufacturing technology for interposer," in *Proc. 5th Electron. Syst.-Integr. Technol. Conf. (ESTC)*, Sep. 2014, pp. 49–51.

[21] Y. Sun, D. Yu, S. Yang, X. Sun, J. Zhang, X. Wei, and L. Wan, "Development of through glass tungsten via interconnect for 3D MEMS packaging," in *Proc. IEEE 13th Electron. Packag. Technol. Conf. (EPTC)*, Dec. 2011, pp. 774–776.

[22] V. Sukumaran, Q. Chen, F. Liu, N. Kumbhat, T. Bandyopadhyay, H. Chan, S. Min, C. Nopper, V. Sundaram, and R. Tummala, "Through-package-via formation and metallization of glass interposers," in *Proc. 60th Electron. Compon. Technol. Conf. (ECTC)*, Jun. 2010, pp. 557–563.

[23] W. L. Stutzman and G. A. Thiele, *Antenna Theory and Design*. Hoboken, NJ, USA: Wiley.

[24] Z. Chen and Z. Shen, "Planar helical antenna of circular polarization," *IEEE Trans. Antennas Propag.*, vol. 63, no. 10, pp. 4315–4323, Oct. 2015.

[25] M. G. Ibambe, Y. Letestu, and A. Sharaiha, "Compact printed quadrifilar helical antenna," *Electron. Lett.*, vol. 43, no. 13, pp. 697–698, Jun. 2007.

[26] Y. Yao, F. Zhang, and F. Zhang, "Microstrip fed planar endfire circularly polarised antenna with enhanced bandwidth," *Electron. Lett.*, vol. 53, no. 7, pp. 445–446, Mar. 2017.

[27] H. T. Hui, K. Y. Chan, and E. K. N. Yung, "The low-profile hemispherical helical antenna with circular polarization radiation over a wide angular range," *IEEE Trans. Antennas Propag.*, vol. 51, no. 6, pp. 1415–1418, Jun. 2003.

[28] A. H. Naqvi, J. H. Park, C.-W. Baek, and S. Lim, "V-band planar helical antenna using TGSV technology," in *Proc. Int. Symp. Antennas Propag. (ISAP)*, Oct. 2018, pp. 1–2.

AQEEL HUSSAIN NAQVI (S'14) received the B.S. degree in electrical engineering from the COMSATS Institute of Information Technology (CIIT), Islamabad, Pakistan, in 2011, and the M.S. degree in electrical engineering from the School of Electrical Engineering and Computer Sciences, National University of Sciences and Technology (NUST), Islamabad, in 2015. He is currently pursuing the Ph.D. degree with the School of Electrical and Electronics Engineering, Chung-Ang University, Seoul, South Korea. His research interests include the design and the analysis of microwave and millimeter-wave antennas, reconfigurable antennas, and planar and 3D printed antennas.

JEONG-HEUM PARK received the B.S. and M.S. degrees from the School of Electrical and Electronics Engineering, Chung-Ang University, Seoul, South Korea, in 2017 and 2019, respectively. His research interests include micro/nanoelectromechanical systems (MEMS/NEMS) and RF/millimeter-wave MEMS devices.

CHANG-WOOK BAEK (S'94–M'95) was born in Anyang, South Korea, in 1970. He received the B.S., M.S., and Ph.D. degrees from the School of Electrical Engineering and Computer Science, Seoul National University, Seoul, South Korea, in 1993, 1995, and 2000, respectively. He was a Postdoctoral Researcher with the Inter-University Semiconductor Research Center (ISRC), Seoul National University, from 2000 to 2002, and as a Research Professor with the School of Electrical Engineering and Computer Science, Seoul National University, from 2002 to 2005. Since 2005, he has been with the School of Electrical and Electronics Engineering, Chung-Ang University, Seoul, South Korea, where he is currently a Professor. He has authored or coauthored over 100 international journals and conference papers in the MEMS research field. His current research interests include micro/nanoelectromechanical systems (MEMS/NEMS), including micro/nanomachining process technologies, RF/millimeter-wave MEMS devices, and micromechanical sensors and actuators. He has served as a Technical Program Committee Member of the IEEE MEMS 2010 and 2011 conferences.

SUNGJOON LIM (S'02–M'06) received the B.S. degree in electronic engineering from Yonsei University, Seoul, South Korea, in 2002, and the M.S. and Ph.D. degrees in electrical engineering from the University of California at Los Angeles (UCLA), Los Angeles, CA, USA, in 2004 and 2006, respectively.

After a postdoctoral position at the Integrated Nanosystem Research Facility (INRF), University of California at Irvine, Irvine, CA, USA, he joined the School of Electrical and Electronics Engineering, Chung-Ang University, Seoul, South Korea, in 2007, where he is currently a Professor. He has authored or coauthored over 250 international conference, letters, and journal papers. His research interests include engineered electromagnetic structures (metamaterials, electromagnetic bandgap materials, and frequency selective surfaces), printed antennas, substrate integrated waveguide (SIW) components, inkjet-printed electronics, and RF MEMS applications. He is also interested in the modeling and the design of microwave circuits and systems.

Prof. Lim received the Institution of Engineering and Technology (IET) Premium Award, in 2009, the ETRI Journal Best Paper Award, in 2014, the Best Paper Award from the 2015 International Workshop on Antenna Technology (iWAT), the Best Paper Award from the 2018 International Symposium on Antennas and Propagation (ISAP), and the CAU Distinguished Scholar, from 2014 to 2018.